Modal properties of unstable resonator semiconductor lasers with a lateral waveguide

J. Salzman, R. Lang, T. Venkatesan,[a] M. Mittlestein, and A. Yariv
128-95 California Institute of Technology, Pasadena, California 91125

(Received 15 April 1985; accepted for publication 13 June 1985)

The modal properties of unstable resonator lasers with a lateral waveguide have been analyzed, and an unstable resonator semiconductor laser with a real index lateral waveguide has been demonstrated. Output powers in excess of 400 mW were observed with a stable, highly coherent lateral field distribution. The incorporation of a lateral real index waveguide with the unstable resonator configuration results in an increase in the external quantum efficiency and the appearance of ripples in the lateral field distribution.

Recently, the fabrication and operation of GaAs heterostructure lasers with an unstable resonator (UR) were reported by us and others.[1–6] It was shown that the unstable resonator geometry is a promising approach for coherent, high-power semiconductor lasers. In these devices, the presence of magnifying mirrors within the cavity continuously defocuses the optical field, thus suppressing filamentation. However, the reported lasers exhibit an external quantum efficiency considerably lower than that of Fabry–Perot lasers due to the high cavity losses. The incorporation of an additional real index lateral waveguide should reduce the diffraction losses of the cavity and lead to a higher external quantum efficiency while maintaining the UR's inherent suppression of filamentation. Here, we report on the fabrication, operation, and analysis of unstable resonator semiconductor lasers with lateral waveguiding. The expected output characteristics and cavity losses of the proposed structure can be obtained by performing a self-consistent modal analysis of this cavity. However, because of the lateral waveguiding effects, the conventional theory of open-walled unstable resonators[7] is not applicable to this case, and a new formalism is needed.

In the present study, the field inside the cavity is analyzed in terms of the waveguide eigenmodes $\{E_n(x)\}$ and the complex mirror reflectivity $R(x)$, where x is the coordinate in the junction plane perpendicular to the mirror (z) axis. The transverse variation (y) can be taken out by making an effective index approximation. The total field propagating along the cavity can be written as

$$E(x,z) = \sum_n a_n E_n(x) e^{-i\beta_n z}, \tag{1}$$

where a_n and β_n are the mode amplitudes and propagation constants, respectively, of the complex index (lateral) waveguide. The set of eigenmodes can be restricted to those discrete confined modes with less loss than the radiation modes (and the radiation modes can be neglected entirely) when the resonator is sufficiently long to ensure near total decay of the neglected modes in one transit of the cavity. Assuming that at $z = 0$, a single mode $E_n(x)$ is incident on the curved mirror, then the reflected field $R(x)E_n(x)$ can be expanded in terms of waveguide modes as

$$R(x)E_n(x) = \sum_m k_{nm} E_m(x), \tag{2}$$

where the $\{k_{nm}\}$ are the elements of a matrix K given by

$$k_{nm} \equiv \int E_n(x)\, R(x)\, E_m(x)\, dx \tag{3}$$

[no conjugation appears in Eq. (3) because the $\{E_n\}$ are already the conjugates of the eigenmodes of the adjoint problem]. The $\{k_{nm}\}$ are thus the mode-coupling coefficients due to the curved mirrors. We represent the incident field at $z = 0$, $\Sigma_n a_n E_n(x)$, by a column vector A with components $\{a_n\}$. After reflection from the mirror, the field is given by

$$\mathbf{A}' = \mathsf{K}\mathbf{A}, \tag{4}$$

where K is the mirror-coupling matrix. The effect of propagation over the distance L in the waveguide is represented by the diagonal matrix $\mathsf{P}(L)$, with $p_{nm} = \delta_{nm} \exp(-i\beta_n L)$.

The eigenmode A of the resonator can be found by requiring that the total field reproduce itself to within a complex constant[8] after one round trip

$$\mathsf{P}(L)\mathsf{K}_2\mathsf{P}(L)\mathsf{K}_1\mathbf{A} = \gamma\mathbf{A}, \tag{5}$$

where the subscripts 1 and 2 refer to the left and right mirrors, respectively. The quantity $|\gamma|^2$ represents the fraction of energy that remains in the cold cavity after one round trip. Consequently, the resonator mode possessing the largest $|\gamma|$ (and thus, the lowest loss) will be the lasing mode.

Equation (5) has been solved for different waveguides (gain guiding, weak and strong index guiding).[8] As expected, the value of $|\gamma|^2$ for gain-guided lasers is close to (but lower than) the inverse of the cavity magnification M.[7] Furthermore, an increase in the index of refraction step reduces the cavity losses $(1 - |\gamma|^2)$. The coupling at the mirrors causes the waveguided modes to be phase locked so that they interfere coherently, producing high (spatial)-frequency ripples in the single lateral mode intensity distribution.

Unstable resonator semiconductor lasers with a lateral waveguide were fabricated on GaAs/GaAlAs separate confinement double heterostructures grown by liquid phase epitaxy. The epilayers were grown on a ⟨111⟩ oriented GaAs substrate. This results in a very uniform crystal growth that manifests itself in low threshold current density for laser operation (in regular 300-μm length Fabry–Perot lasers, as low as 600 A/cm^2). A ridge waveguide, 80 μm wide, was etched in a H_2SO_4:H_2O_2:H_2O (1:8:1) solution down to ~0.3 μm from the active layer (Fig. 1). The additional steps in the device fabrication were identical to those reported in Ref. 5. The lasers were tested with 200-ns pulses at a 1-kHz repeti-

[a] Visiting associate from Bell Communications Research Laboratories, Murray Hill, NJ 07974.

 0003-6951/85/170445-03$01.00

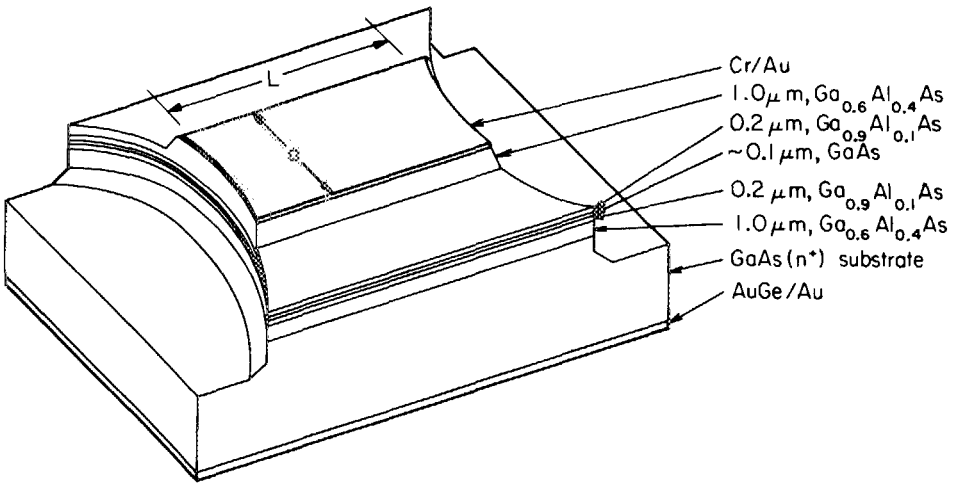

FIG. 1. Schematic drawing of the unstable resonator ridge waveguide laser.

tion rate, and the near-field intensity distribution was observed with an infrared vidicon camera. Figure 2 shows the near-field pattern for three different values of the injection currents. Here, a complicated structure is observed, unlike the case of a gain-guided unstable resonator.[5,6] Note, however, that the field structure remains constant as the current is changed; such would not be the case if random filamentation were occurring.

In Fig. 3, the observed nearfield intensity distribution is recorded, and the calculated intensity is presented for comparison (we estimated an effective index step of $\Delta n = 0.03$). Higher spatial frequencies are visible in the calculated plot than in the experimental plot due to the limited resolution of our viewing system. The ripples are the result of the coherent superposition of the waveguide modes in the (single) resonator mode. To check this point, the spatial coherence of the output field was tested by performing a double slit interference experiment (Young's experiment), as reported before,[6] and high visibility interference fringes [fringe visibility function (FVF) = 0.5–0.6)] were obtained from any two points on the laser facet. This is to be compared with filamentary broad-area lasers, which typically have a fluctuating FVF of < 0.3. The spatial coherence was maintained up to an injection current of $4\,I_{th}$ with an output power of over 400 mW. We assume that, at this point, a second resonator mode was excited.

As stated above, the lateral waveguide reduces the cav-

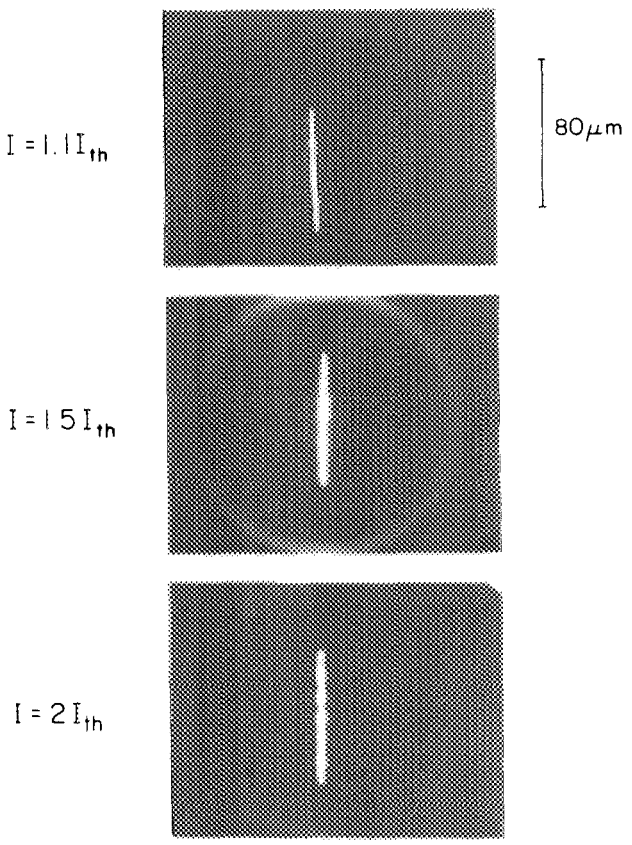

FIG. 2. Near-field pattern for different values of the injection current.

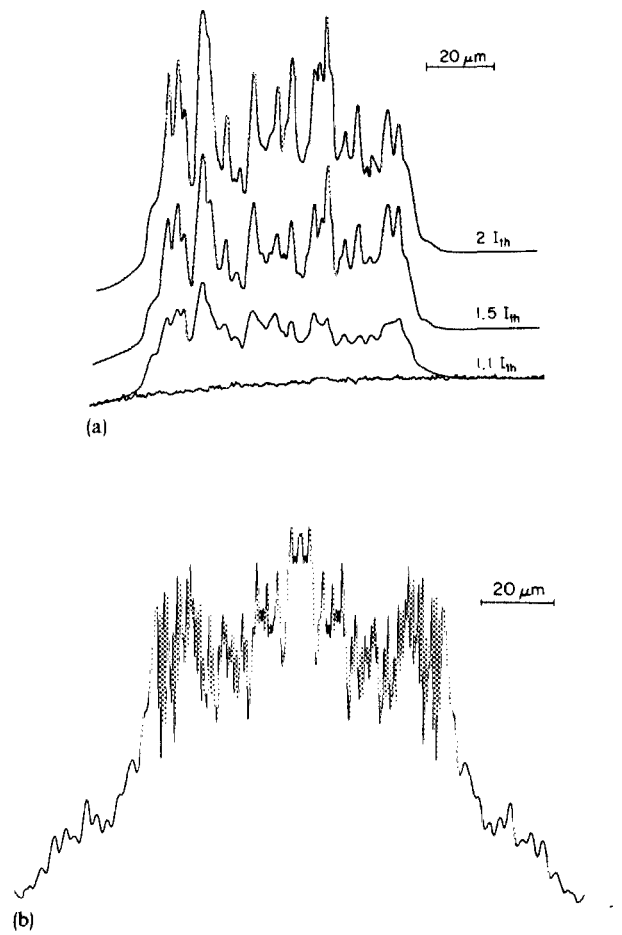

FIG. 3. Near-field intensity distribution; (a) observed and (b) calculated.

TABLE I. Comparison between different broad-area laser geometries.

Laser geometry	Threshold current I_{th} (mA)	External quantum efficiency (η_d)
Broad-area Fabry–Perot (cleaved) laser	250	0.34
Unstable resonator[a]	700	0.22
Ridge waveguide unstable resonator[b]	300	0.28

[a] Ref. 1.
[b] This work.

ity losses by a significant amount. The threshold current and quantum efficiency for the unstable resonator with a lateral waveguide was $I_{th} = 300$ mA and $\eta_d = 0.28$. The external quantum efficiency is related to the mode eigenvalue γ by [8]

$$\frac{1}{\eta_d} = \frac{1}{\eta_i}\left(1 + \frac{\alpha L}{\ln 1/R + \ln 1/|\gamma|}\right)\frac{1-|\gamma|R}{1-R}, \qquad (6)$$

where η_i is the internal quantum efficiency, R is the mirror reflectivity, and α is the absorption loss. In our case, we estimated $|\gamma| \approx 0.5$, leading to $\eta_d = 0.28$, in very good agreement with the measured value. (Note that the threshold current in all semiconductor lasers is affected by an additive term proportional to $-(\ln|\gamma|)/L$, where $|\gamma|$ is any lumped loss.[9] This may result in a dramatic increase in threshold current when compared to the Fabry–Perot case ($|\gamma| = 1$), whereas η_d is reduced only slightly [Eq. (6)]. A comparison between different broad-area laser geometries in terms of I_{th} and η_d is given in Table I. From Table I and the above discussion, we can conclude that the incorporation of a lateral waveguide to the unstable resonator semiconductor laser results in a significant decrease of the cavity losses. The near-field intensity distribution is degraded by ripples that arise from the interference effects between the coupled waveguide modes. Yet, the suppression of filamentation associated with UR's is retained.

In conclusion, the modal properties of unstable resonator lasers with a lateral waveguide have been analyzed in terms of the waveguide eigenmodes, and an unstable resonator semiconductor laser with a real index lateral waveguide has been demonstrated. The results show that the combination of index guiding and an unstable resonator geometry can efficiently produce high optical power in a stable, coherent lateral mode.

This research was supported by grants from the Air Force Office of Scientific Research and the Office of Naval Research. J. Salzman, R. Lang, and M. Mittlestein would like to acknowledge the financial support of the Bantrell Postdoctoral Fellowship and the Fulbright Fellowship, the National Science Foundation, and the German National Scholarship Foundation, respectively.

[1] A. P. Bogatov, P. G. Eliseev, M. A. Man'ko, G. T. Mikaelyan, and Yu. N. Popov, Sov. J. Quantum Electron. **10**, 620 (1980).
[2] R. Craig, L. W. Casperson, G. A. Evans, and J. J. J. Yang, presented at Conference on Lasers and Electro-Optics, Anaheim, CA June 1984.
[3] T. Venkatesan, J. Salzman, R. Lang, M. Mittelstein, and A. Yariv, presented at the Optical Society of America annual meeting, San Diego, Ca, October 1984.
[4] R. R. Craig, L. W. Casperson, O. M. Stafssudd, J. J. J. Yang, G. A. Evans, and R. A. Davidheiser, Electron. Lett. **21** 63 (1985).
[5] J. Salzman, T. Venkatesan, R. Lang, M. Mittlestein, and A. Yariv, Appl. Phys. Lett. **46**, 218 (1985).
[6] M. Mittlestein, J. Salzman, T. Venkatesan, R. Lang, and A. Yariv, Appl. Phys. Lett. **46**, 923 (1985).
[7] A. E. Siegman, Appl. Opt. **13**, 353 (1974).
[8] R. Lang, J. Salzman, and A. Yariv (unpublished).
[9] H. C. Casey, Jr. and M. B. Panish, *Heterostructure Lasers* (Academic, New York, 1978), pp. 181–183.